Supporting Information

A Polyamide-Polyamine Cryptand as Dicarboxylate Receptor: Di-anion Binding Studies in the Solid State, in Solution, and in the Gas Phase

Sourav Chakraborty [a§], Subrata Saha [a§], Luís M. P. Lima[b], Ulrike Warzok[c] , Sayan Sarkar[a], Bidyut Akhuli[a], Mandira Nandi[a], Somnath Bej[a], Nayarassery N. Adarsh[d], Christoph A. Schalley*[c], Rita Delgado*[b], Pradyut Ghosh*[a]

[§] Both authors contributed equally to this work

.[a] Department of Inorganic Chemistry, Indian Association for the Cultivation of Science, 2A & 2B Raja S. C. Mullick Road, Kolkata - 700032, India. Email: icpg@iacs.res.in .

[b]Instituto de Tecnologia Química e Biológica António Xavier, Universidade Nova de Lisboa, Avenida da República, 2780-157 Oeiras, Portugal, Email: delgado@itqb.unl.pt.

[c] Institut für Chemie und Biochemie der Freien Universität Berlin, Takustrasse 3, 14195 Berlin (Germany), Email: c.schalley@fu-berlin.de

[d]Institut Catala de Nanociencia i Nanotecnologia (ICN2), Edifici ICN2, Campus UAB Cerdanyola del Valles, 08193 (Spain).

Table of Contents — **Page No.**

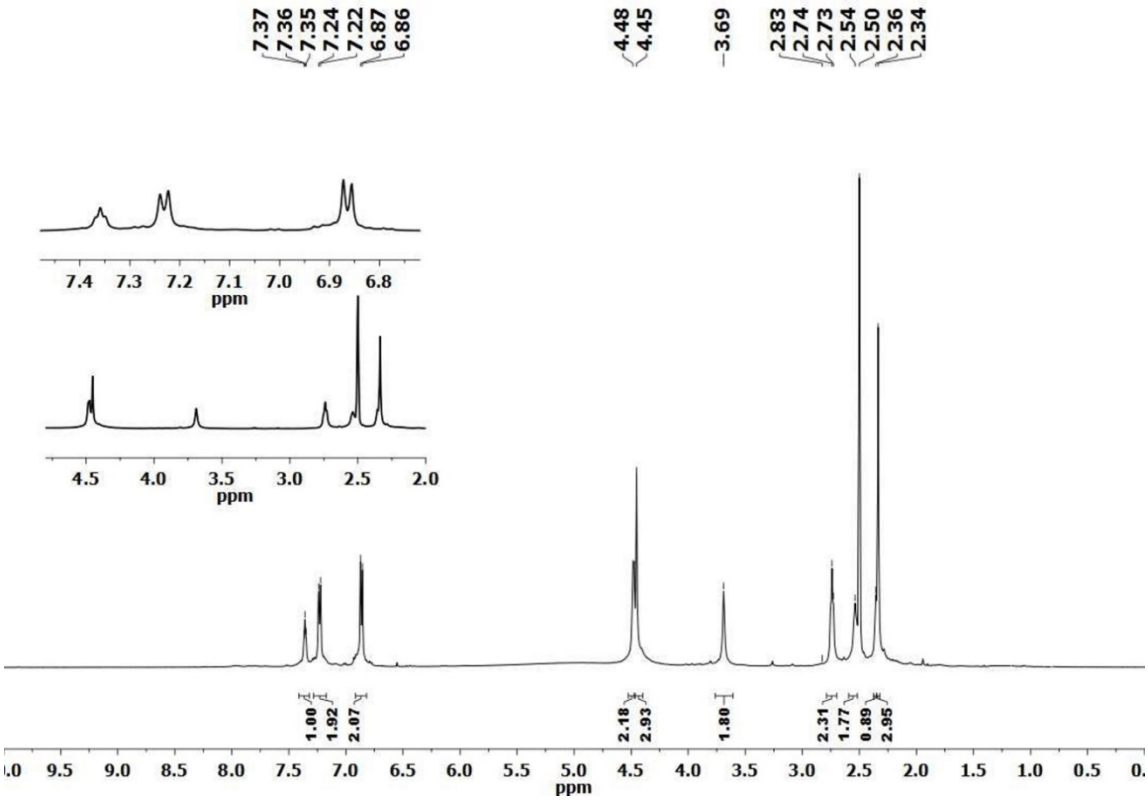

Figure S1: 300 MHz ^{1}H-NMR spectrum of **1** in DMSO-d_6 at 298K.

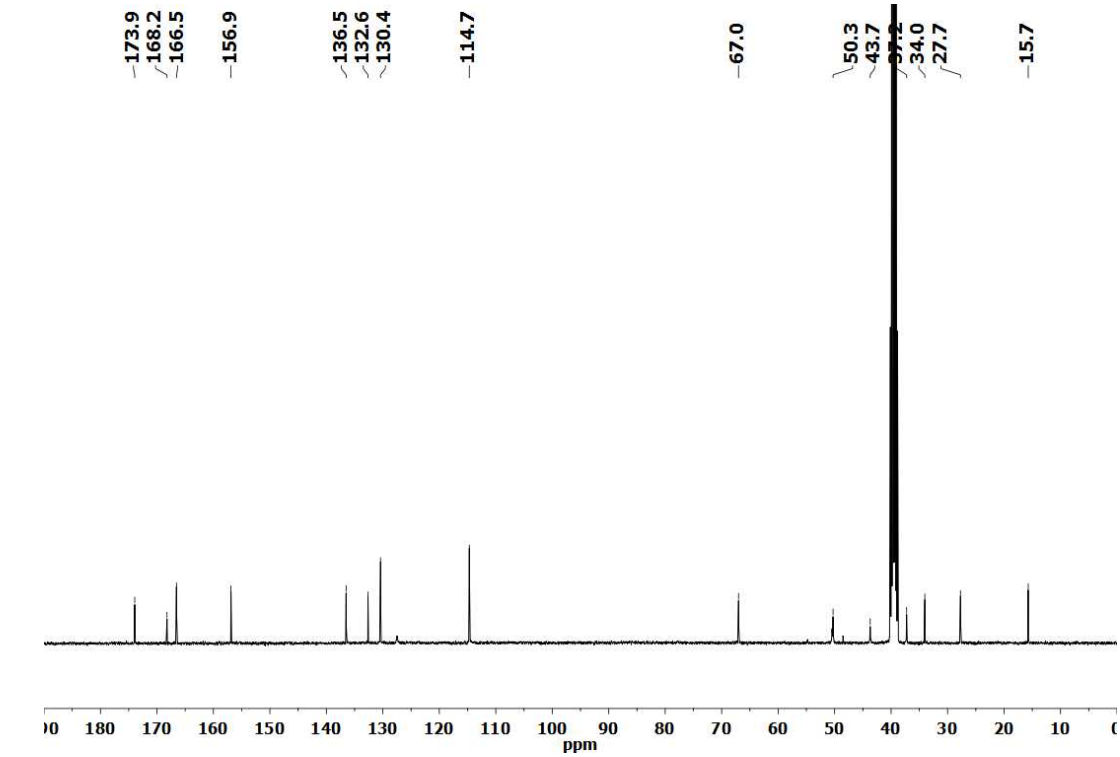

Figure S2: 75 MHz ^{13}C-NMR spectrum of **1** in DMSO-d_6 at 298K.

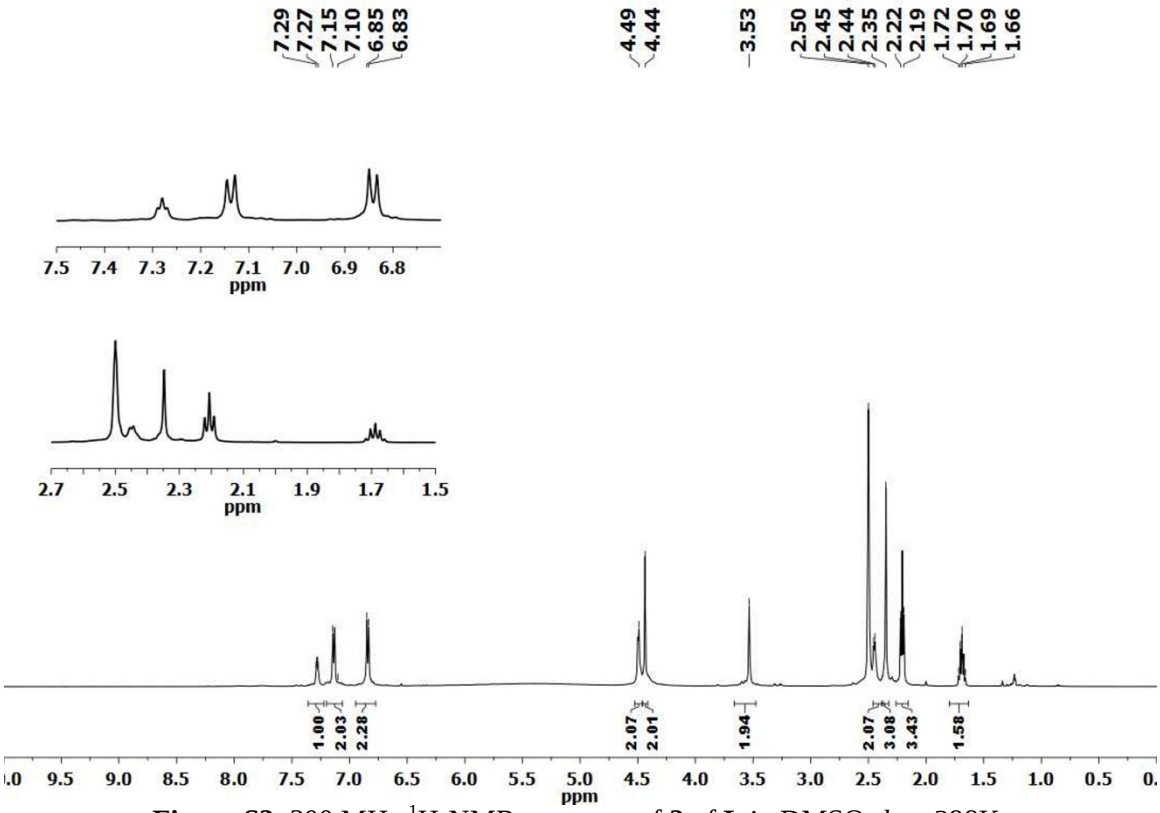

Figure S3: 300 MHz ^{1}H-NMR spectrum of **2** of **L** in DMSO-d_6 at 298K.

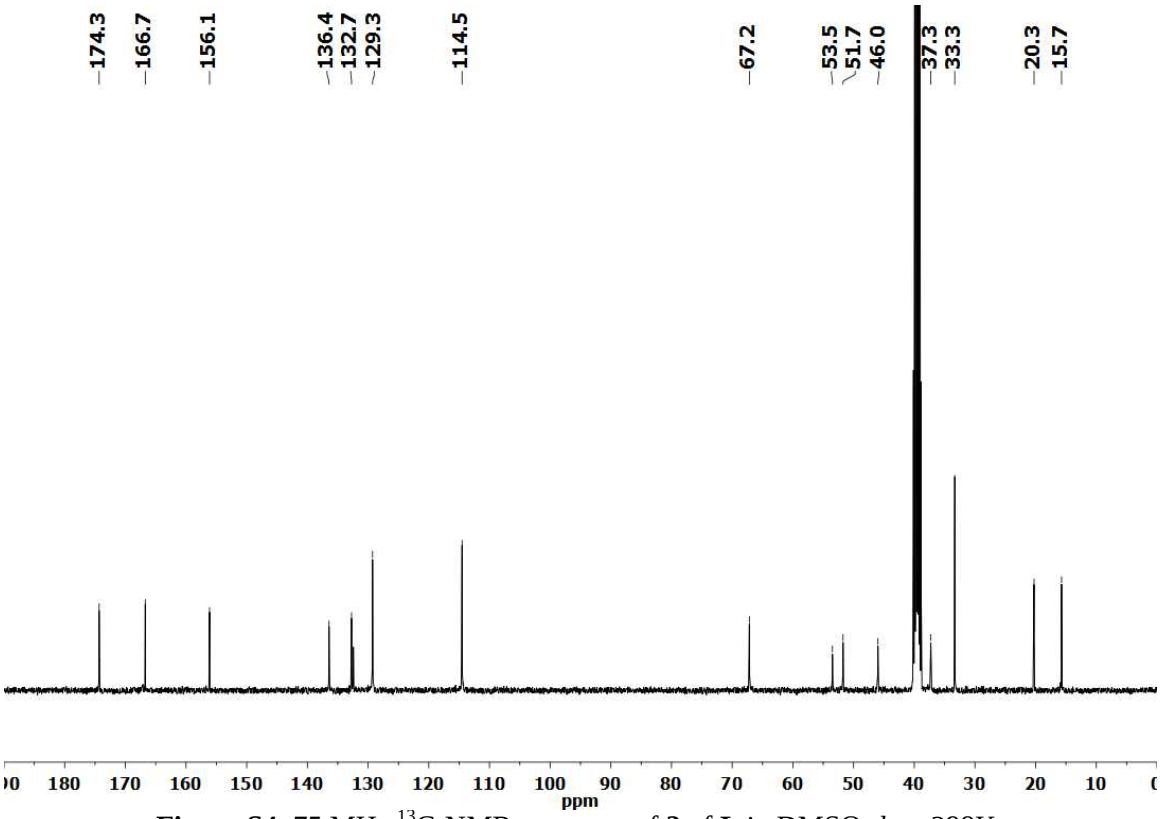

Figure S4: 75 MHz ^{13}C-NMR spectrum of **2** of **L** in DMSO-d_6 at 298K.

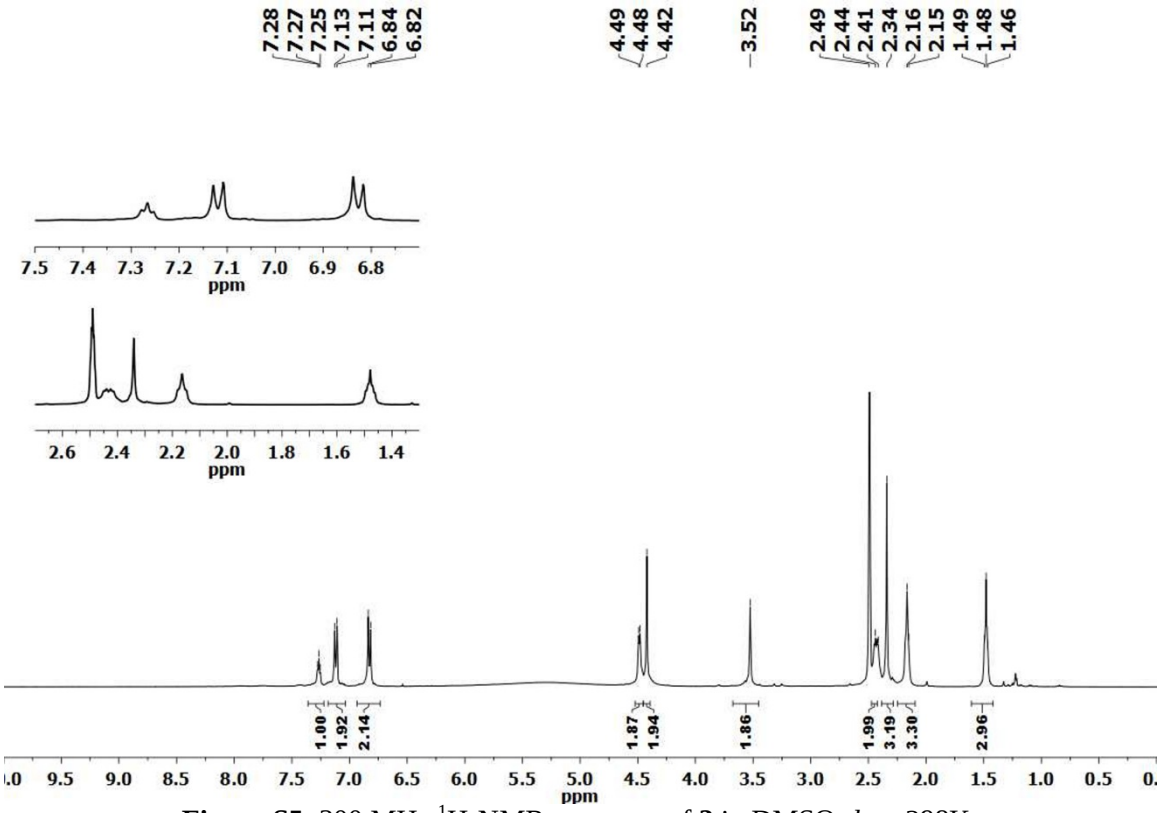

Figure S5: 300 MHz ^{1}H-NMR spectrum of **3** in DMSO-d_6 at 298K.

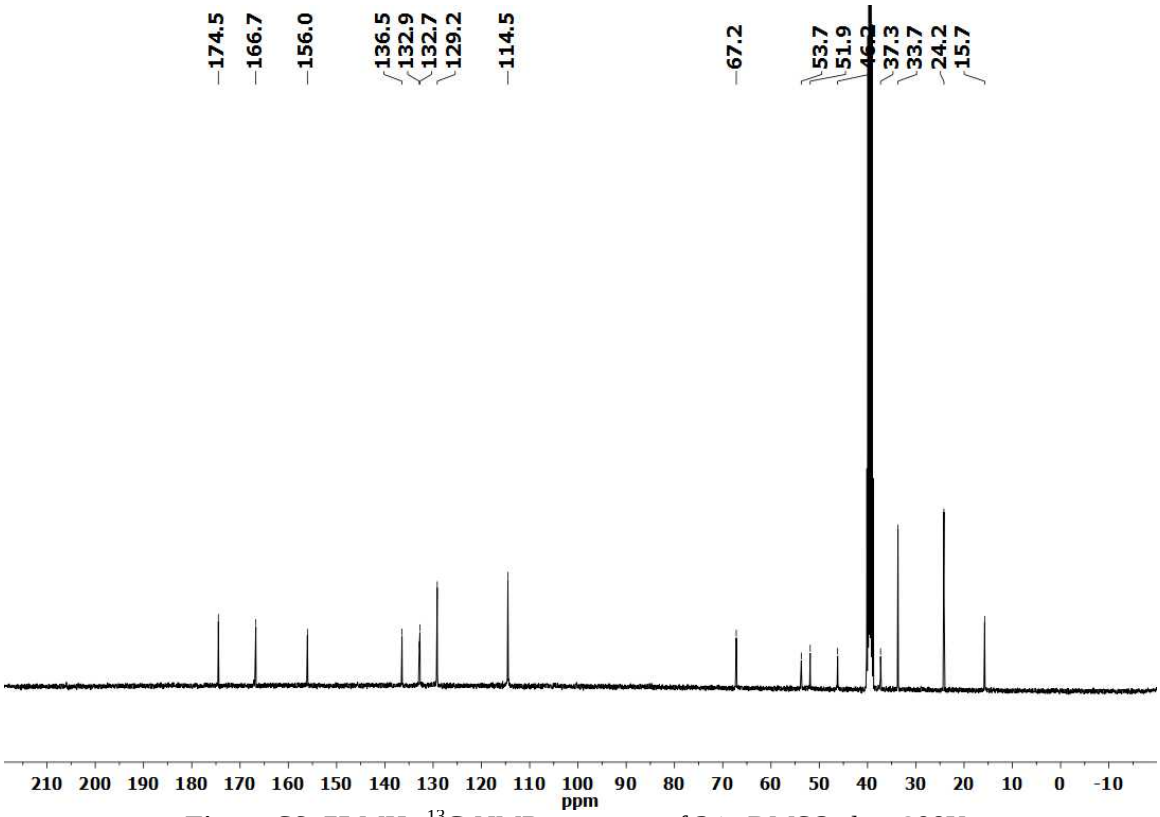

Figure S6: 75 MHz ^{13}C-NMR spectrum of **3** in DMSO-d_6 at 298K.

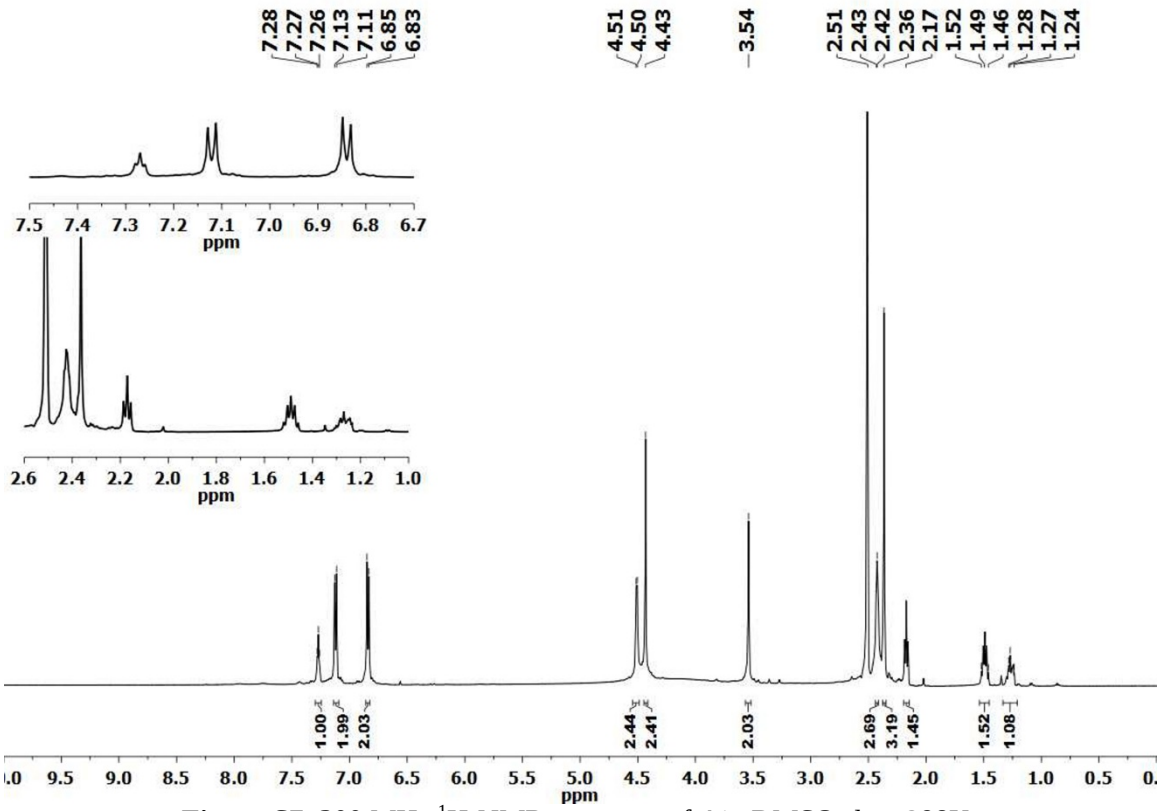

Figure S7: 300 MHz ^{1}H-NMR spectrum of **4** in DMSO-d_6 at 298K.

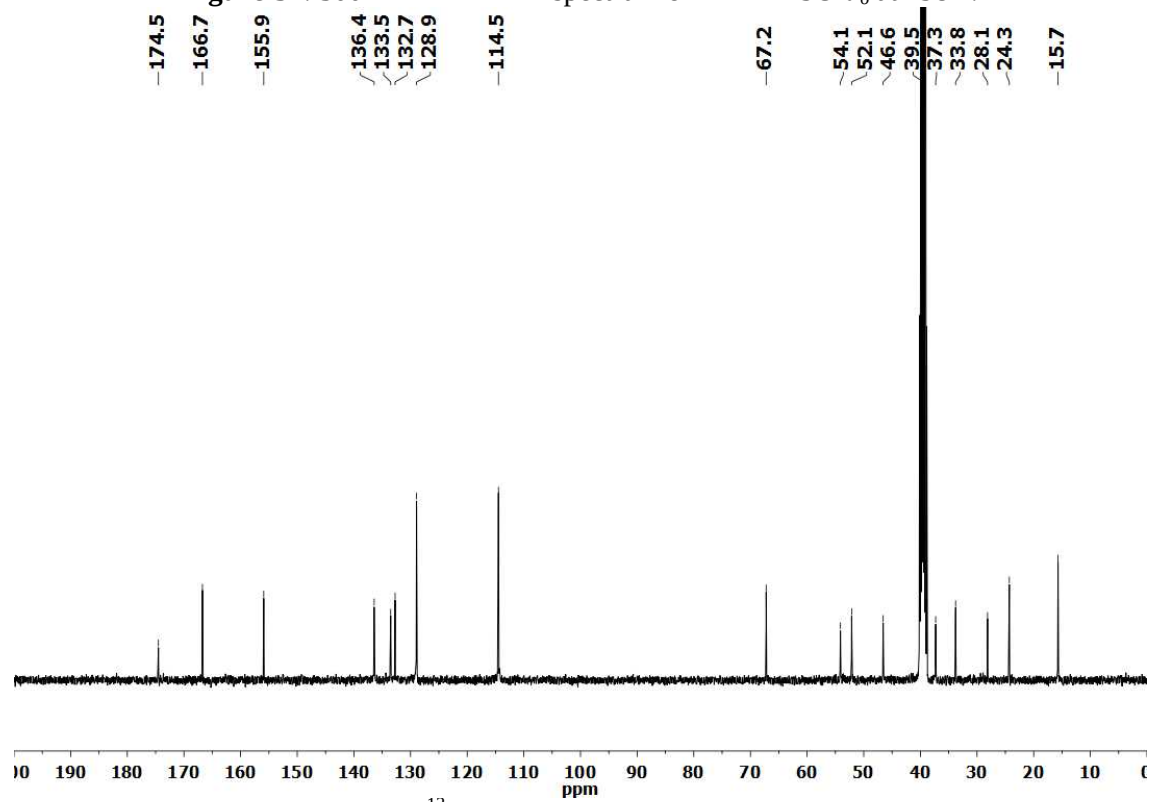

Figure S8: 75 MHz ^{13}C-NMR spectrum of **4** in DMSO-d_6 at 298K.

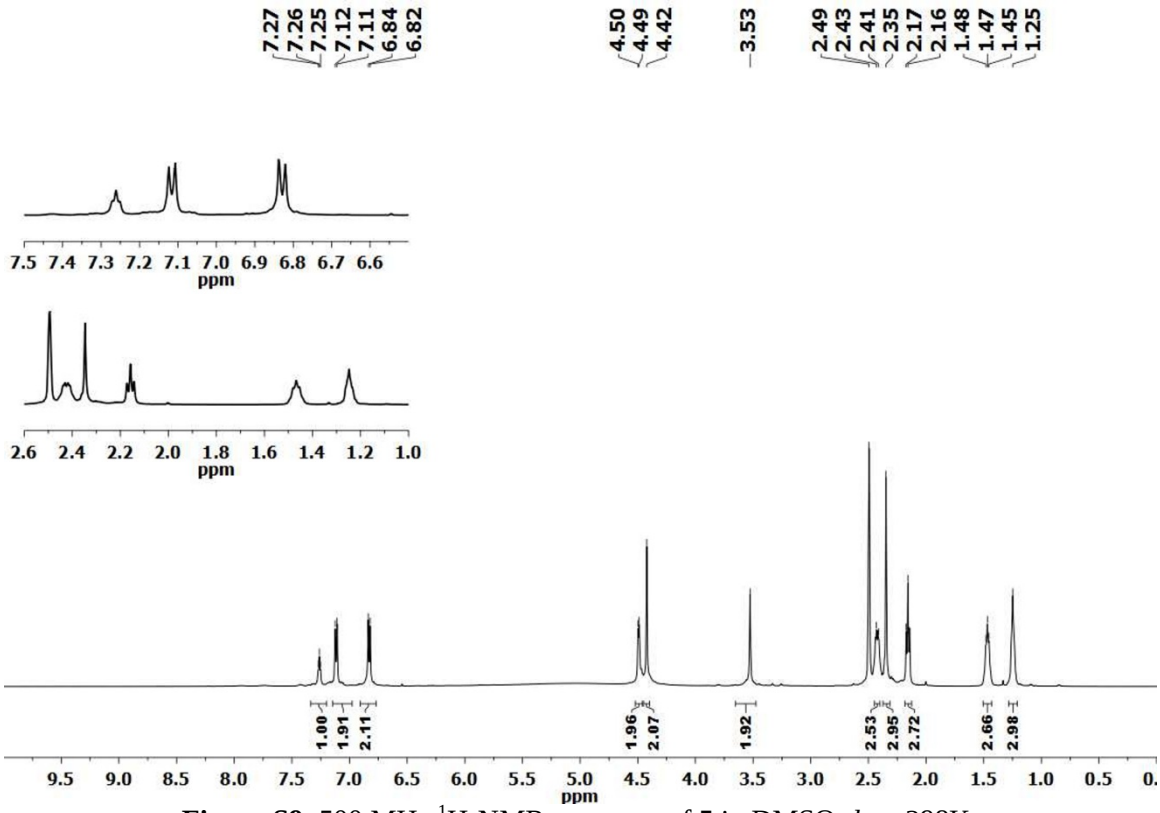

Figure S9: 500 MHz ^{1}H-NMR spectrum of **5** in DMSO-d_6 at 298K.

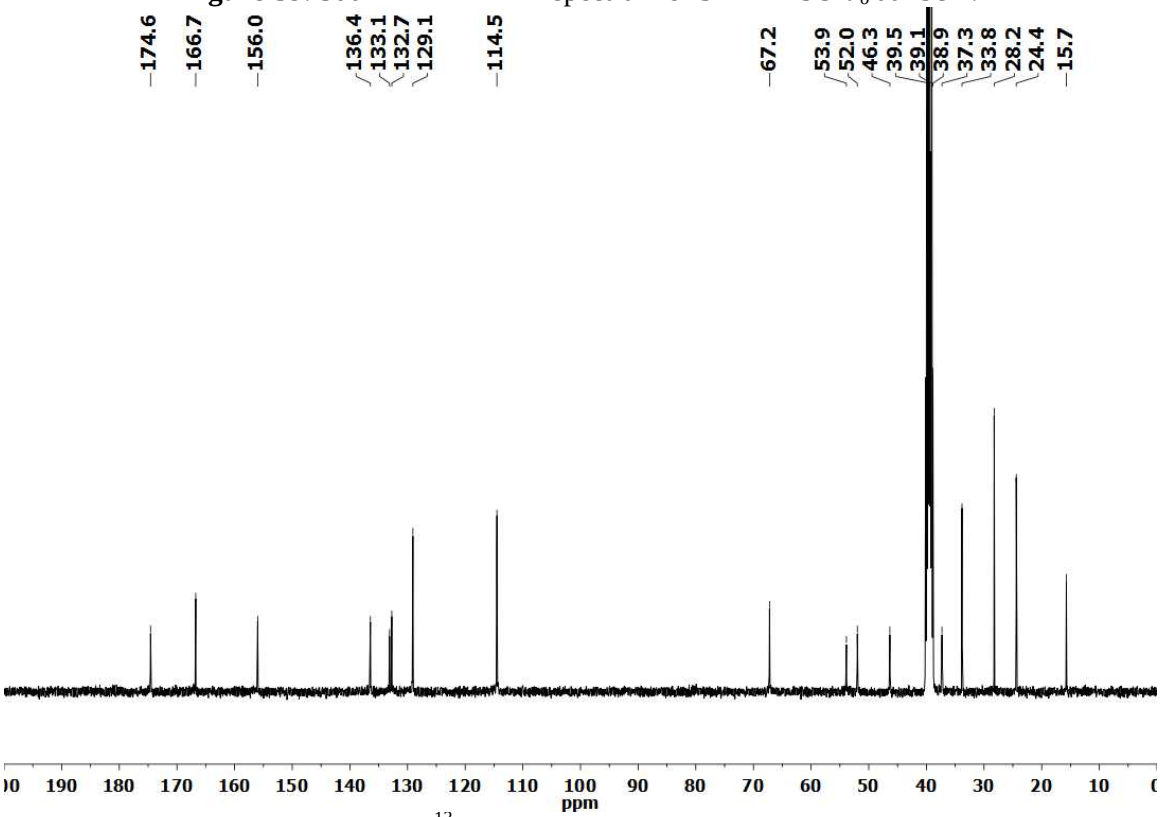

Figure S10: 75 MHz ^{13}C-NMR spectrum of **5** in DMSO-d_6 at 298K.

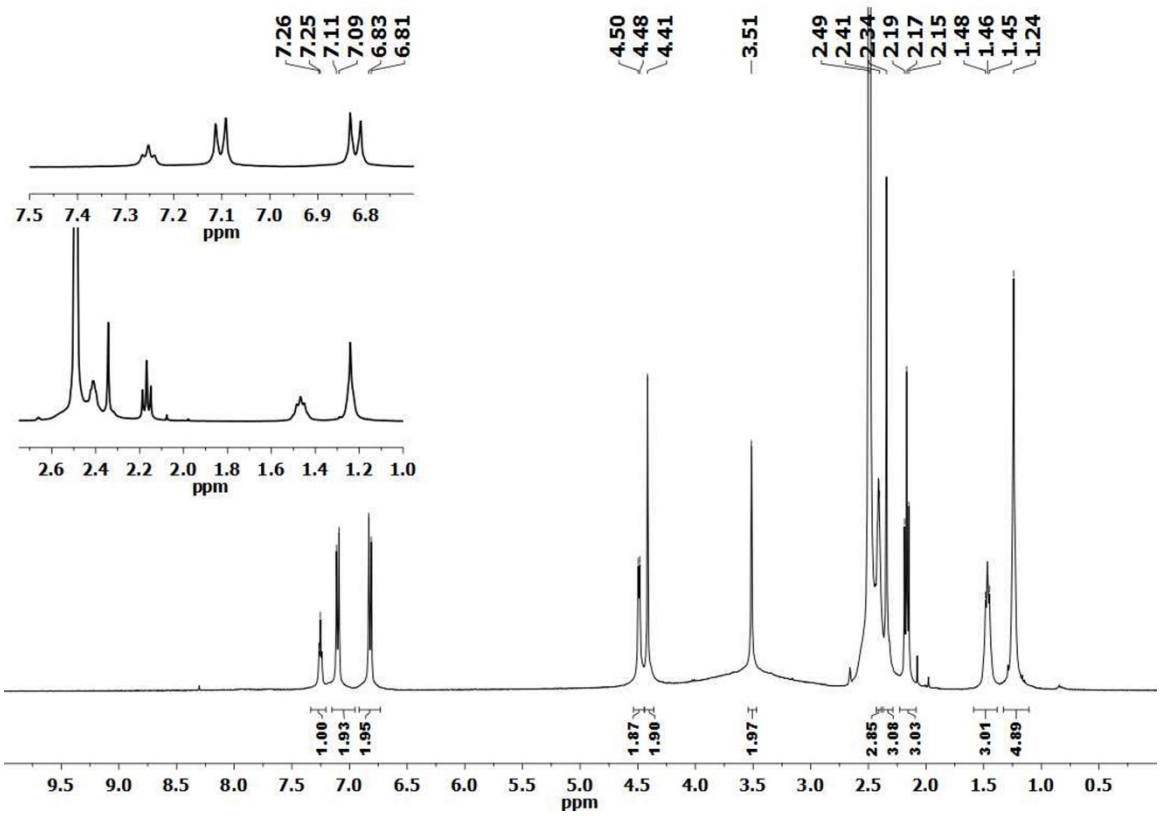

Figure S11: 300 MHz ^{1}H-NMR spectrum of **6** of **L** in DMSO-d_6 at 298K.

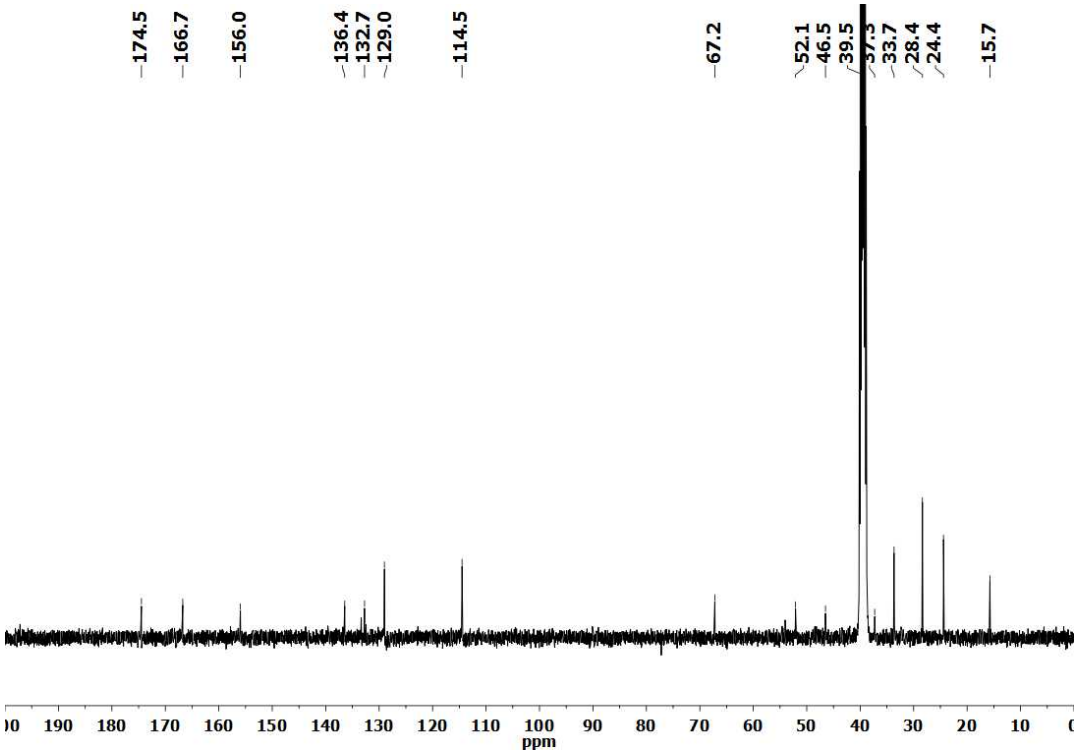

Figure S12: 75 MHz ^{13}C-NMR spectrum of **6** of **L** in DMSO-d_6 at 298K.

Table S1. Overall (log β_{H_hLA}) and stepwise (log K_{H_hLA}) association constants of the protonated species of **L** (H_iL^{i+}) with the various guests (H_2A) in H_2O:DMSO (50:50 v/v) solution at 25.0˚C and I = 0.10 M in $NaClO_4$

Equilibrium reaction	suc^{2-}	glu^{2-}	$kglu^{2-}$	adi^{2-}	pim^{2-}	sub^{2-}	aze^{2-}
	log β_{H_hLA}						
$L + 3\ H^+ + H_2A \rightleftarrows H_5LA^{3+}$	37.84(5)	–	–	–	–	–	–
$L + 3\ H^+ + HA^- \rightleftarrows H_4LA^{2+}$	32.93(3)	31.96(7)	31.77(3)	32.62(2)	32.48(8)	32.16(6)	–
$L + 3\ H^+ + A^{2-} \rightleftarrows H_3LA^+$	26.46(7)	26.15(5)	26.24(4)	27.05(1)	26.44(7)	26.23(4)	26.17(6)
$L + 2\ H^+ + A^{2-} \rightleftarrows H_2LA$	–	19.3(1)	19.67(5)	20.30(2)	19.7(1)	19.31(9)	19.39(9)
$L + H^+ + A^{2-} \rightleftarrows HLA^-$	–	–	11.4(1)	12.45(3)	–	–	–
$L + A^{2-} \rightleftarrows LA^{2-}$	–	–	–	3.21(5)	–	–	–
	log K_{H_hLA}						
$H_3L^{3+} + H_2A \rightleftarrows H_5LA^{3+}$	3.43(5)	–	–	–	–	–	–
$H_3L^{3+} + HA^- \rightleftarrows H_4LA^{2+}$	3.55(3)	2.71(7)	2.94(2)	3.69(2)	3.18(7)	2.82(6)	–
$H_3L^{3+} + A^{2-} \rightleftarrows H_3LA^+$	3.33(6)	3.08(5)	3.11(4)	3.93(1)	3.31(6)	3.10(4)	3.05(6)
$H_2L^{2+} + A^{2-} \rightleftarrows H_2LA$	–	2.4(1)	2.75(5)	3.38(2)	2.7(1)	2.39(9)	2.47(8)
$HL^+ + A^{2-} \rightleftarrows HLA^-$	–	–	2.3(1)	3.33(3)	–	–	–
$L + A^{2-} \rightleftarrows LA^{2-}$	–	–	–	3.21(5)	–	–	–

Table S2. Overall (log β_{H_iL}) and Stepwise (log K_{H_iL}) Protonation Constants of L and of the Dicarboxylate Guests Studied in H_2O:DMSO (50:50 v/v) Solvent Mixture at 25.0 ± 0.1˚ C and I = 0.10 M in $NaClO_4$

Equilibrium reaction	log β_{H_iL}	Equilibrium reaction	log K_{H_iL}
$L + H^+ \rightleftarrows HL^+$	9.125(1)	$L + H^+ \rightleftarrows HL^+$	9.125(1)
$L + 2\ H^+ \rightleftarrows H_2L^{2+}$	16.918(1)	$HL^+ + H^+ \rightleftarrows H_2L^{2+}$	7.793(7)
$L + 3\ H^+ \rightleftarrows H_3L^{3+}$	23.125(1)	$H_2L^{2+} + H^+ \rightleftarrows H_3L^{3+}$	6.207(8)
$L + 4\ H^+ \rightleftarrows H_4L^{4+}$	25.438(2)	$H_3L^{3+} + H^+ \rightleftarrows H_4L^{4+}$	2.31(1)
$suc^{2-} + H^+ \rightleftarrows Hsuc^-$	6.253(1)	$suc^{2-} + H^+ \rightleftarrows Hsuc^-$	6.253(1)
$suc^{2-} + 2\ H^+ \rightleftarrows H_2suc$	11.283(2)	$Hsuc^- + H^+ \rightleftarrows H_2suc$	5.029(2)
$kglu^{2-} + H^+ \rightleftarrows Hkglu^-$	5.712(3)	$kglu^{2-} + H^+ \rightleftarrows Hkglu^-$	5.712(3)
$kglu^{2-} + 2\ H^+ \rightleftarrows H_2kglu$	8.526(5)	$Hkglu^- + H^+ \rightleftarrows H_2kglu$	2.814(4)
$glu^{2-} + H^+ \rightleftarrows Hglu^-$	6.128(1)	$glu^{2-} + H^+ \rightleftarrows Hglu^-$	6.128(1)
$glu^{2-} + 2\ H^+ \rightleftarrows H_2glu$	11.501(1)	$Hglu^- + H^+ \rightleftarrows H_2glu$	5.373(1)
$adi^{2-} + H^+ \rightleftarrows Hadi^-$	6.124(2)	$adi^{2-} + H^+ \rightleftarrows Hadi^-$	6.124(2)
$adi^{2-} + 2\ H^+ \rightleftarrows H_2adi$	11.658(2)	$Hadi^- + H^+ \rightleftarrows H_2adi$	5.532(2)
$pim^{2-} + H^+ \rightleftarrows Hpim^-$	6.168(1)	$pim^{2-} + H^+ \rightleftarrows Hpim^-$	6.168(1)
$pim^{2-} + 2\ H^+ \rightleftarrows H_2pim$	11.791(1)	$Hpim^- + H^+ \rightleftarrows H_2pim$	5.623(1)
$sub^{2-} + H^+ \rightleftarrows Hsub^-$	6.220(2)	$sub^{2-} + H^+ \rightleftarrows Hsub^-$	6.220(2)
$sub^{2-} + 2\ H^+ \rightleftarrows H_2sub$	11.894(1)	$Hsub^- + H^+ \rightleftarrows H_2sub$	5.674(1)
$aze^{2-} + H^+ \rightleftarrows Haze^-$	6.307(2)	$aze^{2-} + H^+ \rightleftarrows Haze^-$	6.307(2)
$aze^{2-} + 2\ H^+ \rightleftarrows H_2aze$	12.033(2)	$Haze^- + H^+ \rightleftarrows H_2aze$	5.726(2)

Travelling-wave ion mobility-mass spectrometry (TW-IMS)

For TW-IMS measurements, a sample solution containing all host-guest complexes was prepared by mixing one equivalent of each acid with eight equivalents of **L**. In Figure 13S is shown the mass spectrum of this mixture as a 30 μM solution in H_2O/MeOH/CH_2Cl_2 95:4:1. It shows clear signals of the known 1:1 host-guest complexes as well as unbound **L** as the deprotonated species and the chloride adduct.

Analysis of *m*/*z versus* drift time plot provides information on the gas phase structure of different species. For **L** without carboxylate guest, two different gas phase structure groups can be assigned. One for the deprotonated **L** species form and one for **L** species with an anion adduct (Figure 14S, bottom). **L**-acid-aggregate form one single group with a linear progression in the *m*/*z versus* drift time plot which implies that they all possess a very similar gas phase structure. This either means that the carboxylate guests are either

all completely encapsulated in the **L** or all sitting outside of the **L** forming side-on host-guest complexes or mere unspecific adducts. This measurement does not allow to conclusively differentiating between these two possibilities.

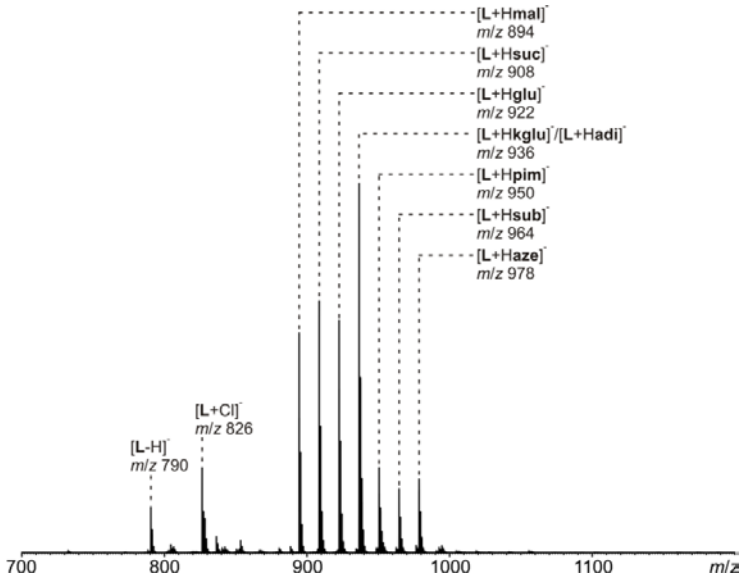

Figure S13: ESI-Q-TOF-HRMS spectra of a mixture of **L** (8 eq.) and malonic acid, succinic acid, glutaric acid. *α*-keto glutaric acid, adipic acid, pimelic acid, suberic acid and azelaic acid (1 eq. each) (30 μM in H_2O/MeOH/CH_2Cl_2 95:4:1).

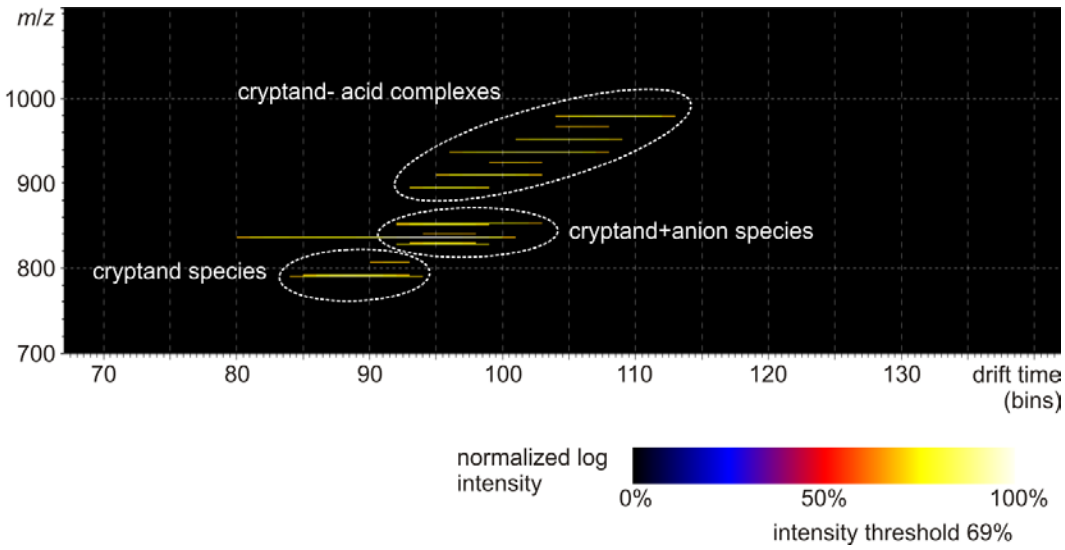

Figure S14: TW-IMS *m/z* versus drift time plot of a mixture of **L** (8 eq.) and malonic acid, succinic acid, glutaric acid. *α*-ketoglutaric acid, adipic acid, pimelic acid, suberic acid and azelaic acid (1 eq. each) (30 μM in H_2O/MeOH/CH_2Cl_2 95:4:1).

Table S3: Crystallographic Details of Host-guest Complexes **1**-**6**.

Complex	**1**	**2**	**3**	**4**	**5**	**6**
Chemical formula	$C_{55}H_{68}N_7O_{24}$	$C_{55}H_{69}N_7O_{24}$	$C_{54}H_{72}N_7O_{29}$	$C_{60}H_{85}N_7O_{24}$	$C_{62}H_{88}N_7O_{16}$	$C_{117}H_{126}N_{14}O_{52}$
Formula Mass	1211.16	1212.17	1283.19	1288.35	1187.39	2560.31
Crystal system	Monoclinic	Monoclinic	Monoclinic	Triclinic	Monoclinic	Triclinic
a/Å	11.8025(7)	38.167(5)	19.851(3)	12.0232(16)	12.685(2)	12.2639(8)
b/Å	20.7261(13)	16.311(2)	14.2576(19)	14.837(2)	17.544(3)	12.7251(8)
c/Å	24.3022(15)	20.656(3)	23.979(3)	21.708(3)	29.713(5)	22.7496(15)
α/°	90.00	90	90.00	100.853(4)	90.00	87.293(2)
β/°	99.226(2)	109.581(4)	101.033(3)	94.193(4)	104.402(7)	87.843(2)
γ/°	90.00	90	90.00	107.650(4)	90.00	79.827(2)
Unit cell volume/Å^3	5867.9(6)	12116(3)	6661.4(15)	3589.0(8)	6404.7(18)	3489.0(4)
Temperature/K	150(2)	150(2)	150(2)	150(2)	150(2)	150(2)
Space group	*P*2(1)/*c*	*C*2/*c*	*P*2(1)/*c*	$P\bar{1}$	*P*2(1)/*c*	$P\bar{1}$
No. of formula units per unit cell, *Z*	4	8	4	2	4	1
No. of reflections measured	53893	72069	66825	34912	20937	32642
No. of independent reflections	7544	11041	13423	7722	4311	11824
R_{int}	0.0910	0.0870	0.0832	0.0407	0.0931	0.0332
Final R_1 values ($I > 2\sigma(I)$)	0.0587	0.0753	0.0900	0.1095	0.0620	0.1078
Final $wR(F^2)$ values ($I > 2\sigma(I)$)	0.1646	0.1969	0.2396	0.3387	0.1498	0.3369
Final R_1 values (all data)	0.0981	0.1299	0.1357	0.1344	0.0901	0.1367
Final $wR(F^2)$ values (all data)	0.2100	0.2219	0.2672	0.3671	0.1664	0.3703
Goodness of fit on F^2	1.029	1.024	1.088	1.620	1.072	1.463
CCDC number						

Table S4: Hydrogen Bonding Parameters of the Host-guest Complexes**1**-**6**

Complex **1**					
D–H···A	D–H (Å)	H···A (Å)	D···A (Å)	D–H···A (^{0})	Symmetry operation for A
N(1)–H(1)···O(7)	0.86	2.25	3.044(5)	154	x, y, z
N(3)–H(3)···O(8)	0.86	2.28	3.052(5)	150	x, y, z
N(4)–H(4A)···O(9)	0.90	2.01	2.883(5)	163	x, y, z
N(5)–H(5D)···O(5)	0.90	1.87	2.725(5)	158	2-x, -1/2+y, 1/2-z
Complex **2**					
N(2)–H(2A)···O(205)	0.89	1.88	2.705(5)	154	x, y, z
N(2)–H(2B)···O(98)	0.89	2.21	2.841(6)	128	x, y, z
N(5)–H(5D)···O(5)	0.89	2.33	3.205(11)	166	x, y, z
N(4)–H(4A)···O(201)	0.89	2.40	3.055(4)	131	x, 1-y, 1/2+z
N(4)–H(4A)···O(208)	0.89	2.13	2.908(5)	145	3/2-x, 1/2-y, 2-z
N(4)–H(4B)···O(99)	0.89	2.07	2.853(12)	146	x, y, z
N(6)–H(6A)···O(63B)	0.89	1.70	2.546(7)	159	x, -1+y, z
N(6)–H(6A)···O(62B)	0.89	2.14	2.819(7)	132	1-x, -1+y, 3/2-z
N(6)–H(6B)···O(98)	0.89	1.86	2.621(7)	142	x, y, z
Complex **3**					
N(2)–H(2B)···O(29)	0.90	1.90	2.799(4)	173	1-x, -1/2+y, 1/2-z
N(4)–H(4B)···O(99)	0.90	1.86	2.749(4)	168	x, y, z
N(6)–H(6)···O(2)	0.86	2.07	2.892(5)	161	x, y, z
N(7)–H(7)···O(1)	0.86	2.02	2.857(4)	163	x, y, z
Complex **4**					
N(3)–H(3)···O(3B)	0.86	2.17	2.991(8)	161	x, y, z
N(5)–H(4B)···O(7D)	0.90	2.43	3.12(2)	134	x, y, z
N(5)–H(4B)···O(9D)	0.90	1.81	2.68(3)	165	x, y, z

N(6)–H(5D)···O(1C)	0.90	1.91	2.805(6)	173	-1+x, y, z
N(6)–H(5D)···O(2C)	0.90	2.50	3.047(7)	119	-1+x, y, z
N(6)–H(5E)···O(2B)	0.90	2.09	2.922(7)	154	x, y, z
N(2)–H(6A)···O(5D)	0.90	1.84	2.738(7)	176	x, y, z
N(2)–H(6B)···O(8D)	0.90	1.91	2.758(6)	156	1-x, 2-y, 1-z
O(4B)–H(10)···O(2C)	0.82	1.81	2.498(9)	141	x, y, z
O(3C)–H(14A)···O(1B)	0.82	1.74	2.549(8)	167	x, -1+y, z
N(5)–H(50G)···O(4D)	0.90	1.94	2.753(11)	149	x, y, z
Complex **5**					
N(2)–H(2)···O(15)	0.86	2.17	2.993(8)	160	x, y, z
N(3)–H(3)···O(12)	0.86	2.36	3.119(7)	148	1-x, -1/2+y, 3/2-z
N(4)–H(4A)···O(11)	0.90	1.84	2.733(7)	175	1+x, y, z
N(4)–H(4B)···O(16)	0.90	1.92	2.758(7)	155	1-x, -1/2+y, 3/2-z
N(5)–H(5A)···O(16)	0.90	1.87	2.761(7)	172	1-x, -1/2+y, 3/2-z
N(5)–H(5B)···O(8)	0.90	1.78	2.675(7)	171	x, y, z
N(6)–H(6A)···O(8)	0.90	1.78	2.674(8)	172	x, y, z
N(6)–H(6B)···O(11)	0.90	1.84	2.699(7)	157	1+x, y, z
O(15)–H(15)···O(12)	0.82	1.91	2.724(7)	170	1-x, -1/2+y, 3/2-z
Complex **6**					
N(5)–H(5A)···O(21)	0.89	1.85	2.650(7)	148	x, y, z
N(5)–H(5A)···O(115)	0.89	2.60	3.196(8)	125'	1-x, -y, 1-z
N(5)–H(5B)···O(90)	0.89	1.99	2.843(6)	160	x, -1+y, z
N(5)–H(5A)···O(21)	0.89	2.49	3.043(6)	121	x, y, z
N(6)–H(6A)···O(93)	0.89	2.02	2.807(6)	146	x, y, z
N(6)–H(6B)···O(101)	0.89	2.09	2.96(2)	166	x, y, z
N(7)–H(7A)···O(101)	0.89	1.90	2.78(2)	174	1-x, -y, 1-z

N(7)–H(7A)···O(116)	0.89	1.84	2.73(2)	177	1-x, -y, 1-z
N(7)–H(7B)···O(90)	0.89	1.89	2.769(5)	169	x, -1+y, z

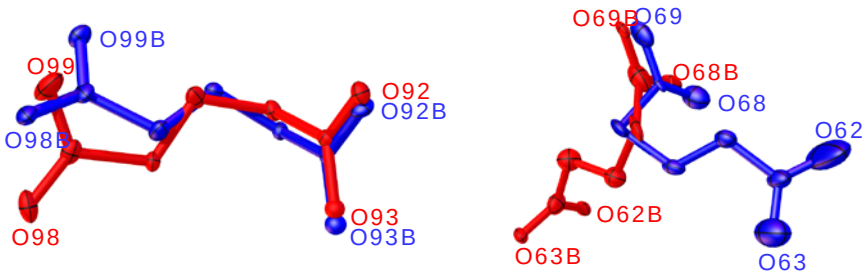

Figure S15: The two position disorder of glutarate carboxylate anion in **2**.

Packing of host-guest complexes 1-6 through hydrogen bonding (Figure S16-S21)

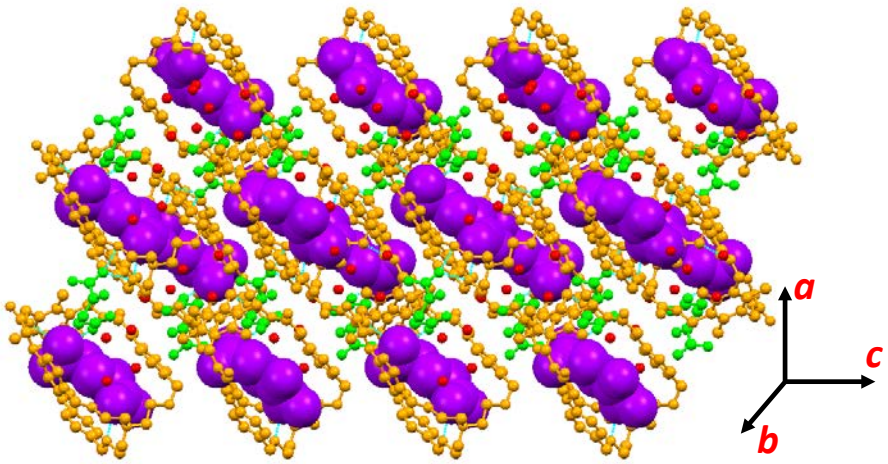

Figure S16: Packing of **1** stabilized by 3D hydrogen bonding involving protonated macrobicycle (orange), encapsulated α-ketoglutarate ion (purple), non-encapsulated α-ketoglutarate ion (green) and lattice included water molecules (red), along crystallographic axis “b”.

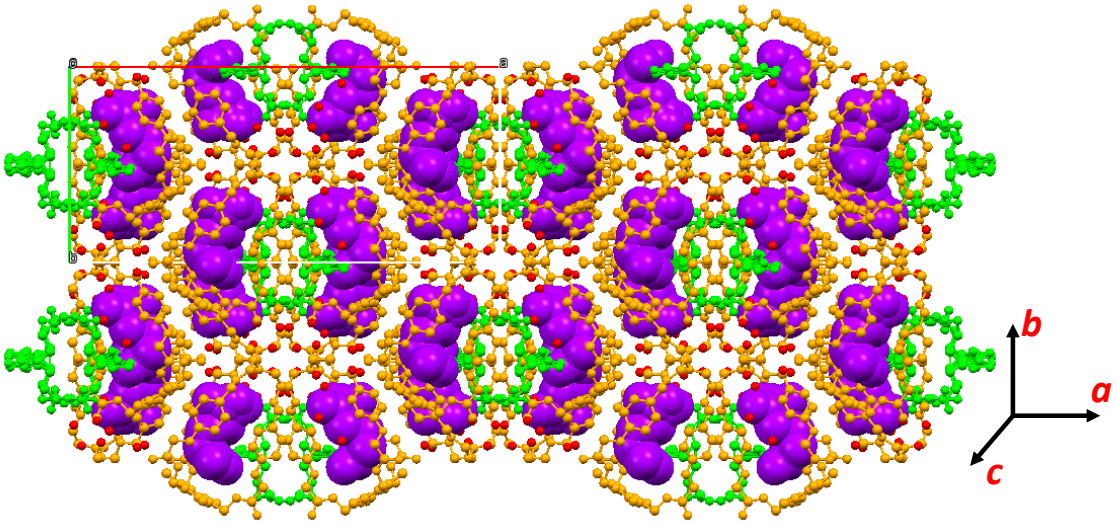

Figure S17: Overall packing of **2**, displaying the 3D hydrogen bonding involving protonated macrobicycle (orange), encapsulated glutarate ion (purple), non-encapsulated glutarate ion (green) and lattice included water molecules (red), view along crystallographic axis “c”.

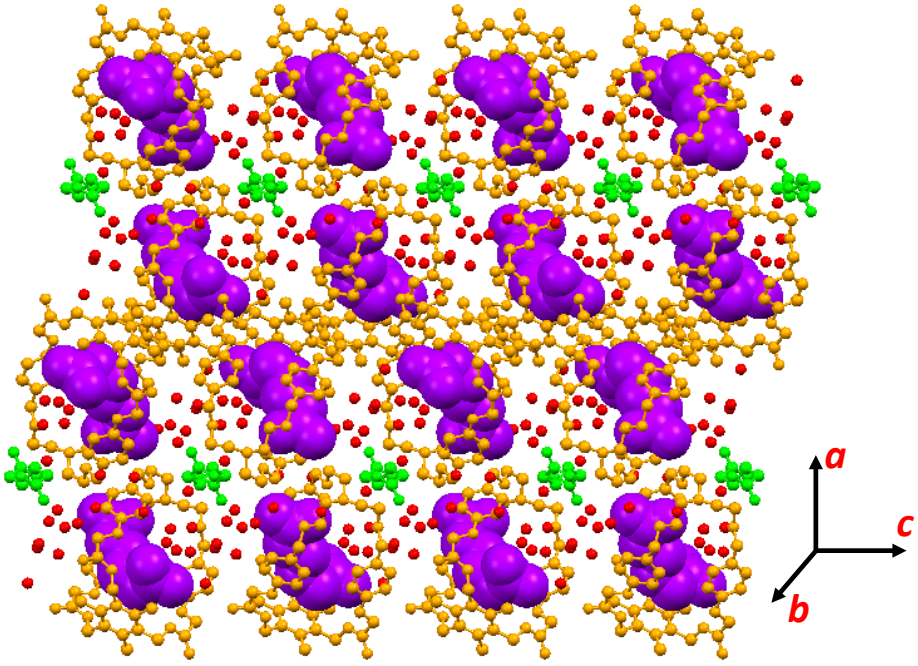

Figure S18: Packing diagram of **3**, in which the protonated macrobicycle (orange), encapsulated adipate ion (purple), non-encapsulated adipate ion (green) and lattice included water molecules (red) were involved in various hydrogen bonding interactions, view along crystallographic axis “b”.

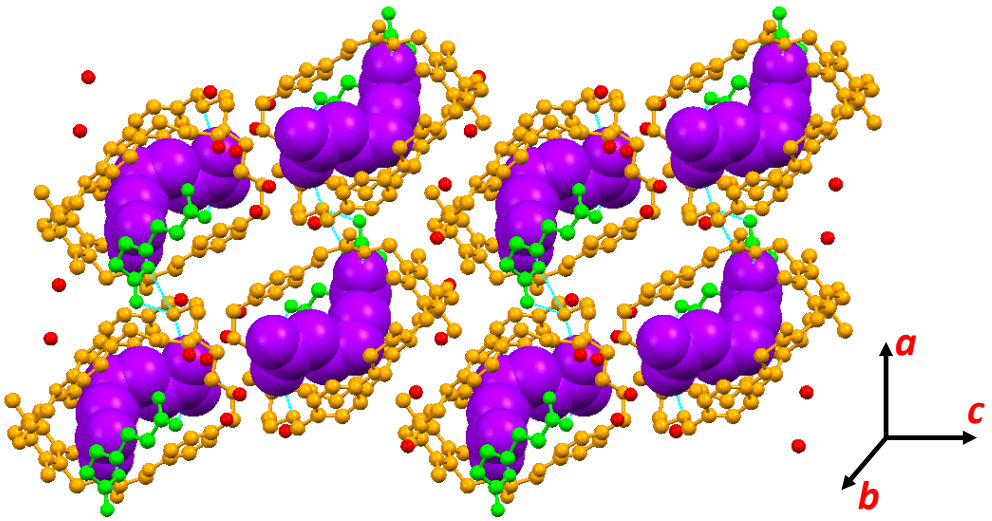

Figure S19: Parallel packing of 1D hydrogen bonded chain in **4** [macrobicycle (orange), encapsulated pimelate ion (purple), non-encapsulated pimelate ion (green) and lattice included water molecules (red)], view along crystallographic axis "b"

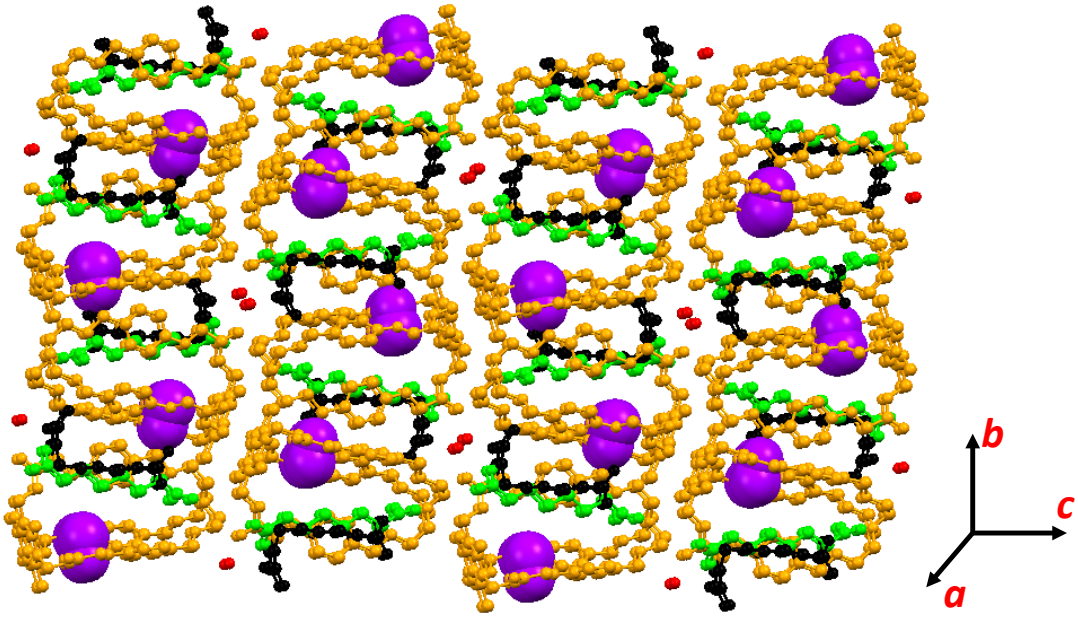

Figure S20: Overall packing in **5**, displaying the encapsulation of MeOH (purple) within the cavity of macrobicycle (orange). The non-encapsulated suberate ions (green and black) and lattice included water molecules also shown. All components are involving various hydrogen bonding interaction. View along crystallographic axis "a".

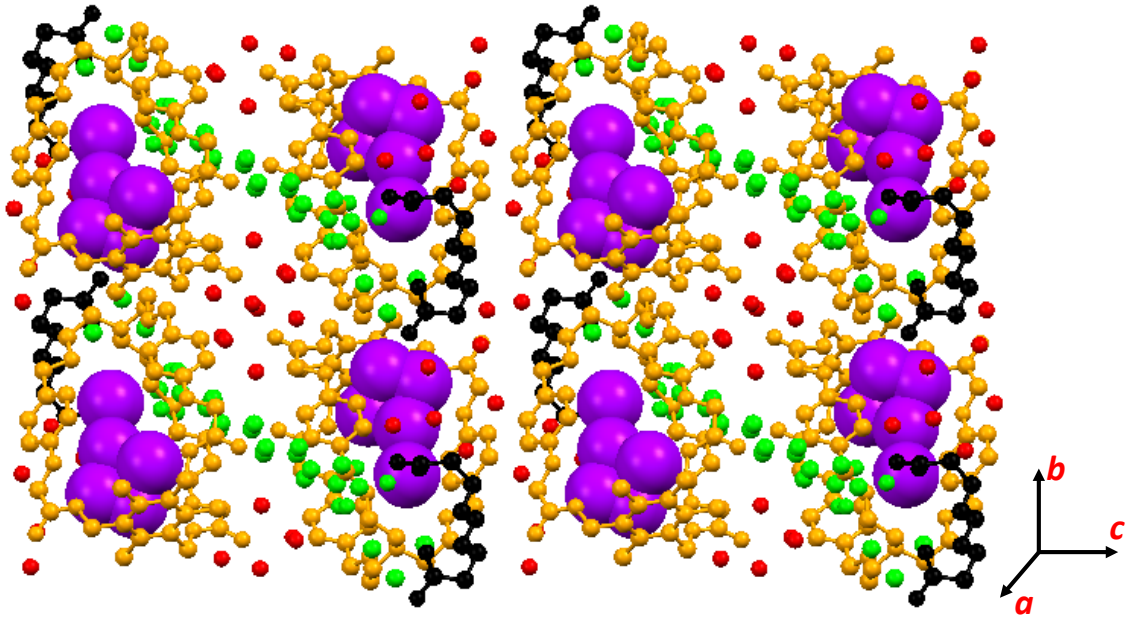

Figure S21: Overall packing in **6**, displaying the encapsulation of water molecules (purple) within the cavity of macrobicycle (orange). The non-encapsulated azelate ions (green and black) and lattice included water molecules (red) also shown. All components are involving various hydrogen bonding interaction. View along crystallographic axis "b".

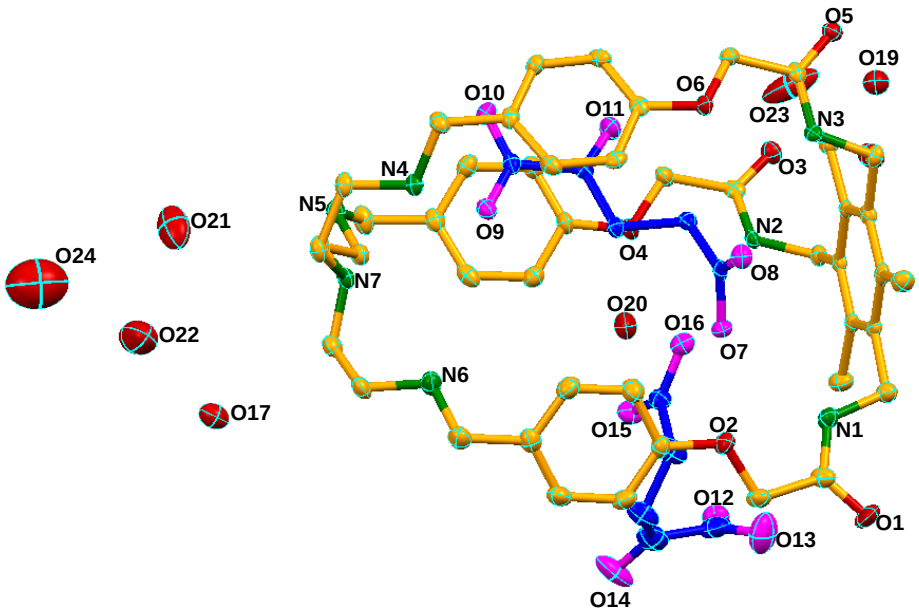

Figure S22: Thermal ellipsoid plots (50% probability level) of compex **1**

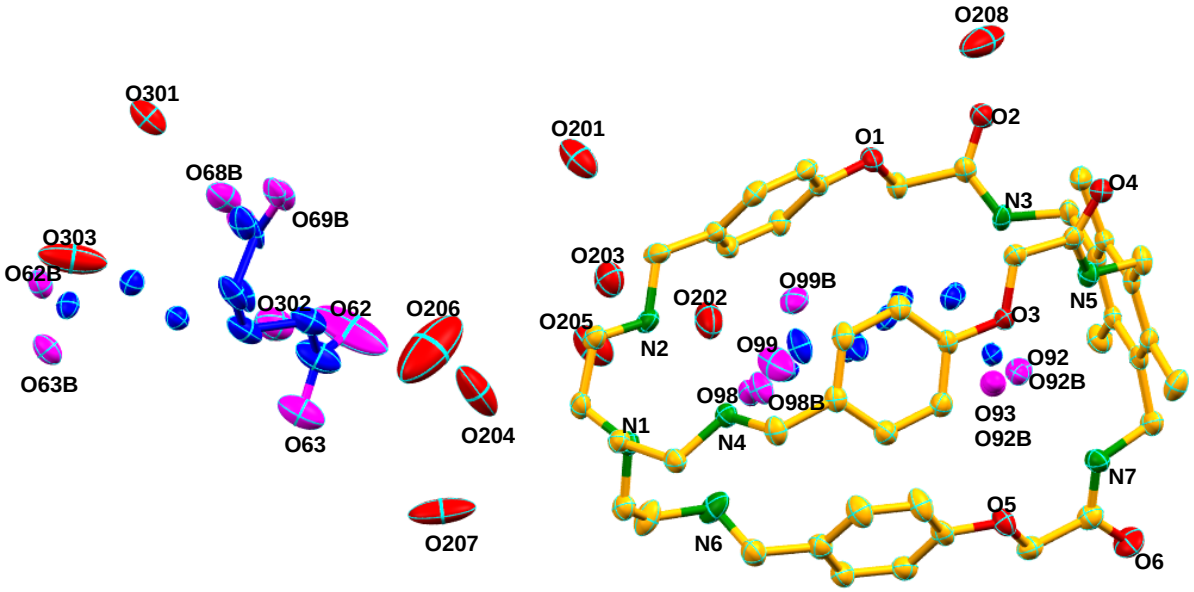

Figure S23: Thermal ellipsoid plots (50% probability level) of compex **2**

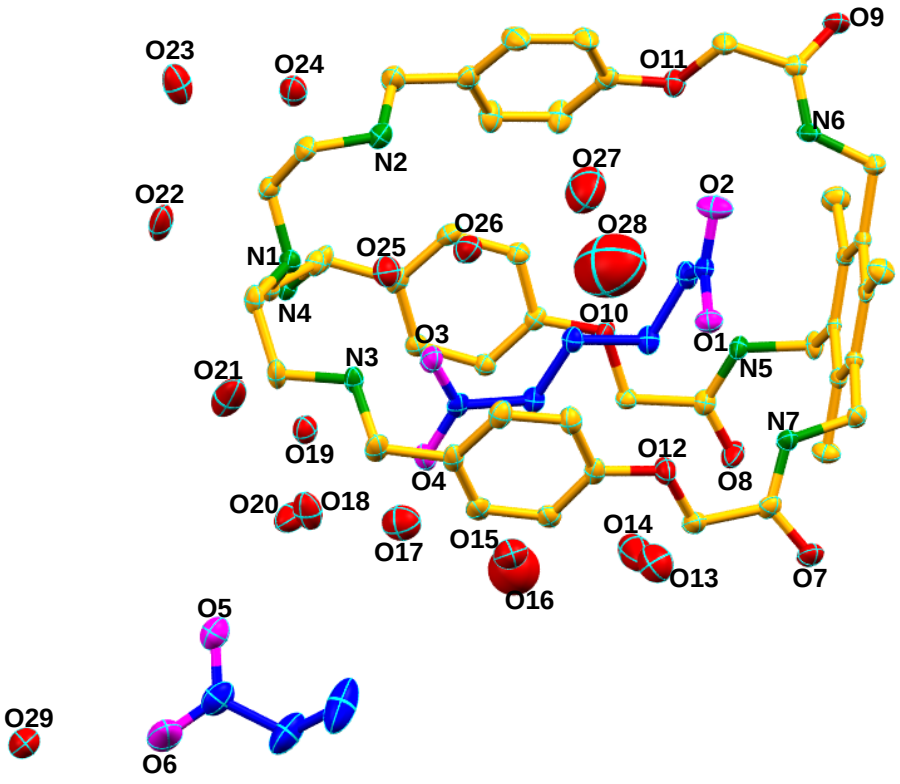

Figure S24: Thermal ellipsoid plots (50% probability level) of compex **3**

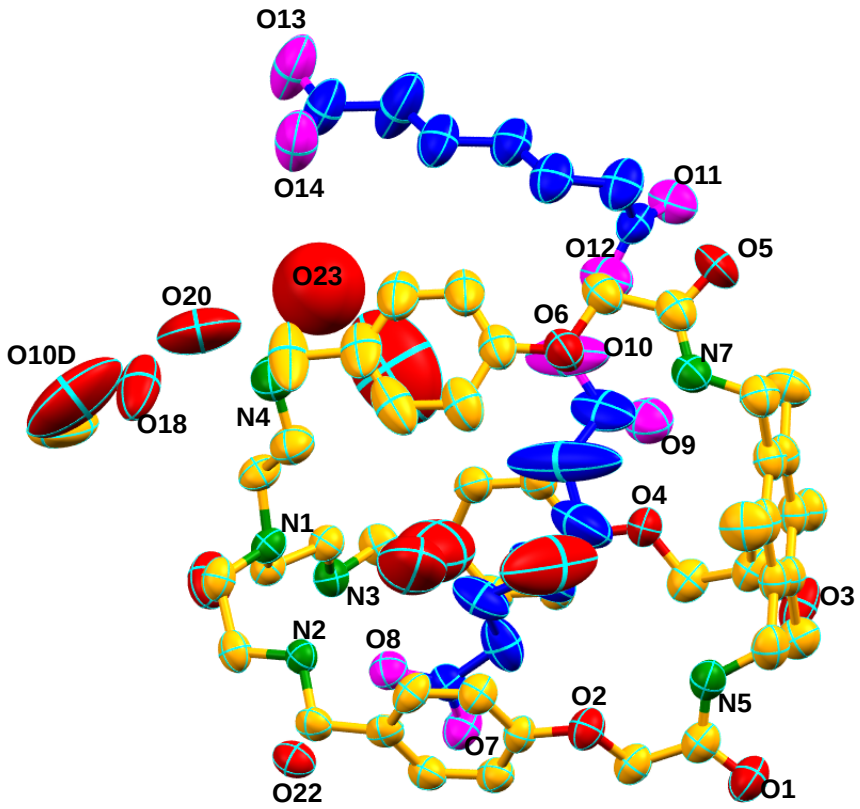

Figure S25: Thermal ellipsoid plots (50% probability level) of compex **4**

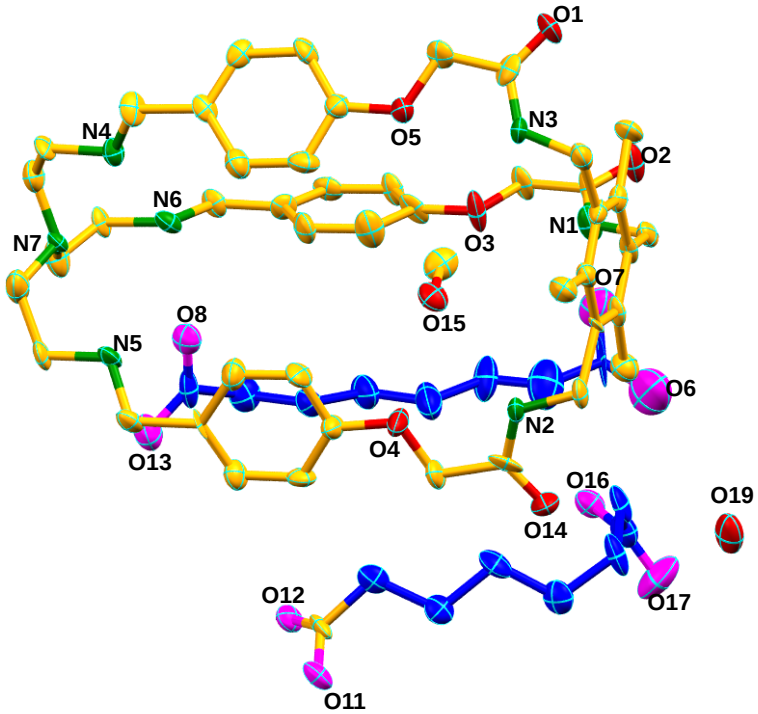

Figure S26: Thermal ellipsoid plots (50% probability level) of compex **5**

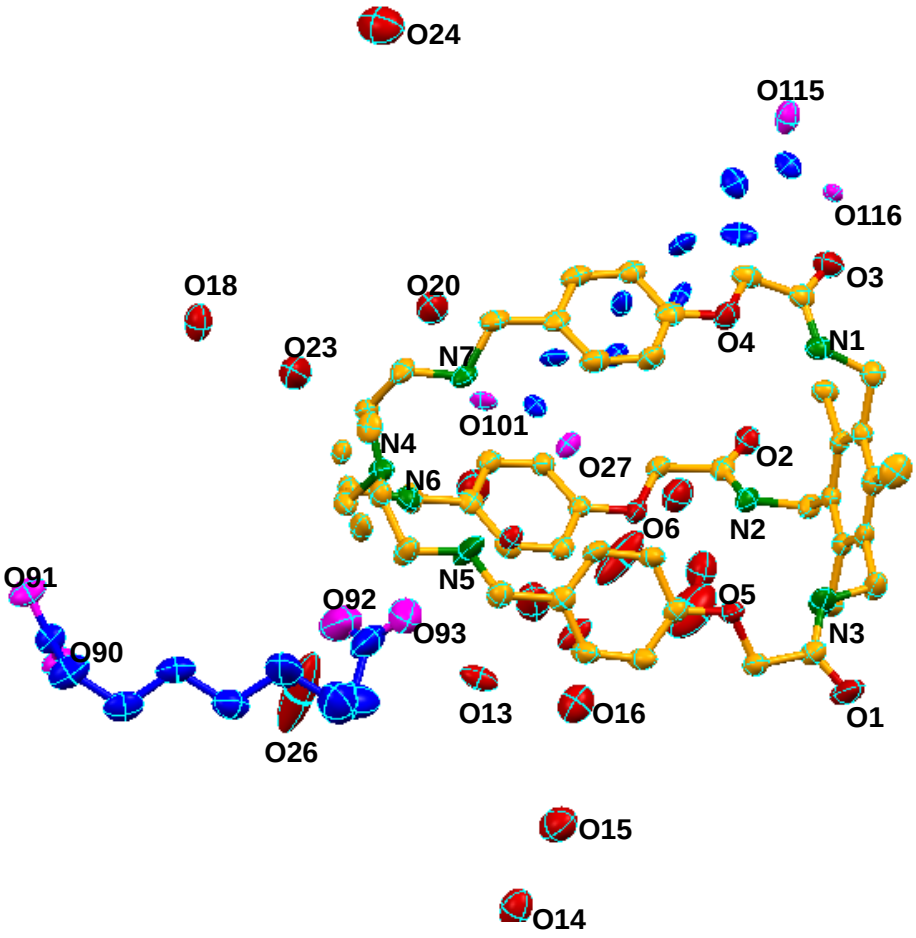

Figure S27: Thermal ellipsoid plots (50% probability level) of compex **6**